

In-Situ Regrowth and Purification by Zone Melting of Organic Single-Crystal Thin Films Yielding Significantly Enhanced Optoelectronic Properties

Chong-Yang Liu and Allen J. Bard*

Department of Chemistry and Biochemistry, The University of Texas at Austin,
Austin, Texas 78712

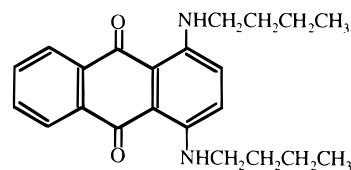
Received May 1, 2000. Revised Manuscript Received June 19, 2000

Amorphous or polycrystalline films of three organic materials (solvent blue 35 and two porphyrins) have been recrystallized into single-crystal thin films (of micrometer thickness) by a zone-melting technique, in which an electrically heated wire generated a narrow molten zone (0.5–2 mm wide) on the organic layer sandwiched between two pieces of glass or indium–tin oxide-coated glass. When the molten zone was moved slowly (3–120 $\mu\text{m}/\text{min}$) across the layer from one end of the cell to the other, a single-crystal film was produced after a single pass. After this treatment, the steady-state short-circuit photocurrent was improved by several orders of magnitude.

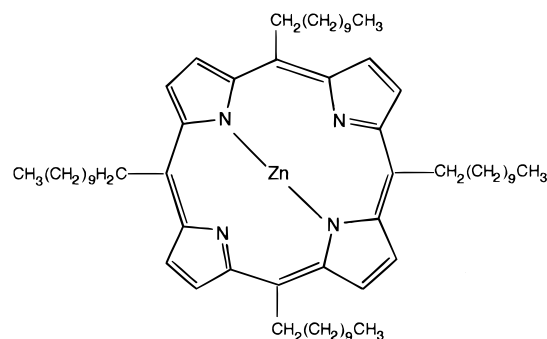
Introduction

We report here a zone-melting technique for the growth and purification of organic single-crystal films within thin-layer ($\sim 1 \mu\text{m}$ thick) sandwich cells for three different compounds: 1,4-bis(butylamino)-9,10-anthraquinone (solvent blue 35 or SB35), zinc(II) meso-5,10,15,20-tetrakis-*n*-undecylporphyrin (porphyrin 1) and zinc(II) 2,3,7,8,12,13,17,18-octa-*n*-decylporphyrin (porphyrin 2). SB35 is a flat molecule with two transition dipole moments along the long and short molecular axes.^{1,2} Porphyrins 1 and 2 have four and eight long hydrocarbon chains, respectively. With this zone-melting procedure, amorphous films and polycrystalline needles (with diameters at the nanometer level) were recrystallized into millimeter-sized single-crystal thin films, and the short-circuit photocurrent (I_{sc}) was improved by up to several orders of magnitude. Such an externally controlled nonepitaxial growth of organic single-crystal thin films should be useful in improving the performance of organic film optical and electronic devices.

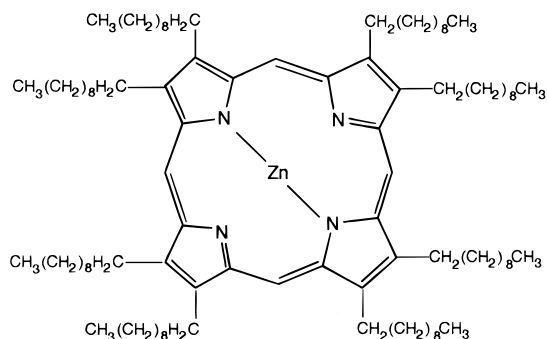
Single crystals of high perfection and purity are desirable when studying the intrinsic properties of solid-state substances.^{3,4} This has been achieved for many inorganic materials, such as Si and GaAs. In fact, the modern electronics industry benefited substantially from an enormous effort toward the growth and purification of silicon single crystals. In addition, our understanding of the fundamental properties of a solid (e.g., structural, electronic, and optical properties) depends strongly on the crystal quality. Progress in this



solvent blue 35



porphyrin 1



porphyrin 2

area for organic molecular crystals has been limited mainly due to certain intrinsic characteristics of the

(1) Saito, T.; Liu, C.-Y.; Bard, A. J. *Chem. Mater.* **1997**, *9*, 1318.

(2) Thulstrup, E. W.; Michl, J. *Elementary Polarization Spectroscopy*; VCH: New York, 1989.

(3) Karl, N. In *Crystals, Growth, Properties, and Applications*; Freyhardt, H. C., Ed.; Springer-Verlag: Heidelberg, 1980; Vol. 4, pp 1–100.

(4) Lawson, W. D.; Nielsen, S. *Preparation of Single Crystals*; Butterworth: London, 1958.

molecules and their constituent solids. For example, the large spacing and weak interactions among neighboring molecules in a crystal make it relatively easy for foreign molecules to be incorporated into the lattice, often leading to an impure crystal with many defects.⁵ A high-temperature annealing process to improve the crystal quality and purity (by allowing impurities to diffuse out), which is effective for inorganic solids, is not available for most organic crystals because of their low melting points and poor thermal stability. On the other hand, organic molecules generally have strong optical absorption coefficients, so thin films (of micrometer thickness) are required for characterization of their optoelectronic properties. The orientational dependence of light absorption of many molecules can only be studied with single crystals. To our knowledge, no externally controllable technique for the growth of single-crystal, micrometer-thick films exists, although ordered ultrathin films (approximately in the nanometer range) can be prepared by Langmuir–Blodgett deposition,⁶ from self-assembled mono- and multilayers in solution, and more recently by organic molecular beam epitaxy in an ultrahigh vacuum chamber.⁷ We previously demonstrated that several organic single-crystal thin films can be prepared in sandwich cells, i.e., two pieces of indium–tin oxide (ITO)-coated glass spaced about 1–2 μm apart, by capillary filling of the molten organic compound^{8,9} (e.g., porphyrin,¹⁰ sudan I,¹¹ and solvent green 3¹). However, many other materials form only amorphous or polycrystalline films when using the same procedure. Moreover, the purity of most organic films does not approach that characteristic of inorganic solid-state electronic materials. Therefore, we have investigated a zone-melting technique for direct use with the sandwich cells to convert amorphous and polycrystalline films into single-crystal films with higher purity and improved properties.

Experimental Section

SB35 (~98% purity) was purchased from Aldrich and used as received. Porphyrins 1 and 2 were synthesized and purified as described previously.¹² Microscope cover glass (~130–170 μm thick, Fisher Scientific) and ITO (Delta Technologies) were employed as substrates. The symmetrical sandwich cells containing an organic layer were fabricated by a method reported earlier.^{8–10} Briefly, the organic powders were placed at the opening of the empty cells, which were then filled by capillary action with the molten compounds (Figure 1a). Cells of glass/organic layer/glass could be easily made to any thickness and were used primarily for the initial optimization of the experimental conditions for the single-crystal growth; ITO/organic layer/ITO cells (~1.5–2.5 μm thick) were used for the optoelectronic characterizations.

The apparatus of the zone-melting technique is schematically shown in Figure 1b. Cells were placed on an electric heating wire of Pt (diameter, 50, 127, or 250 μm ; 99.99%

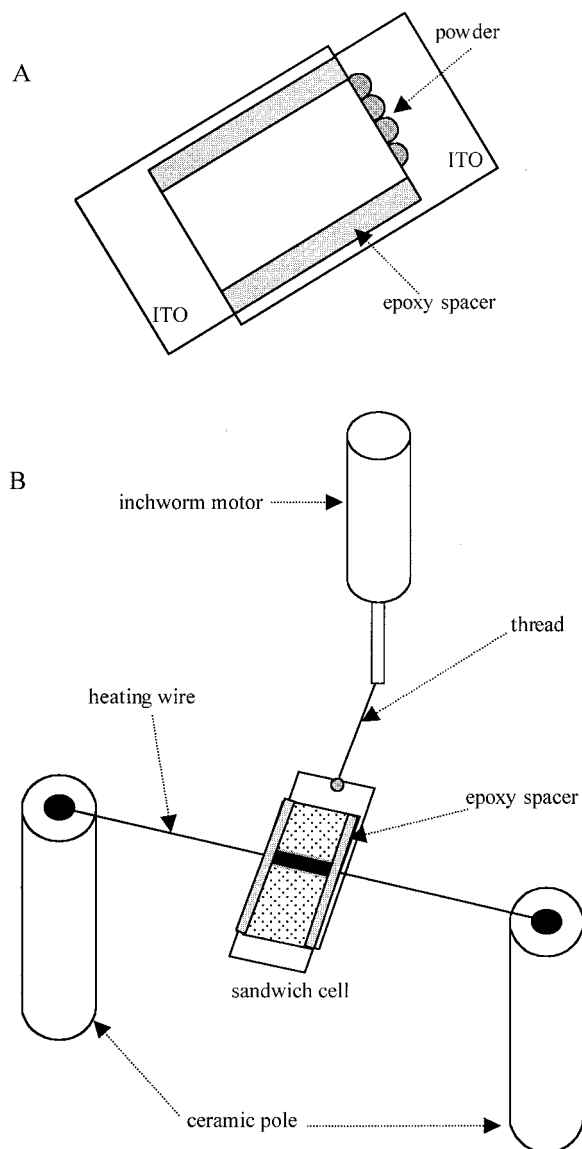


Figure 1. (a) Schematic diagram for the preparation of an ITO/organic film/ITO sandwich cell and (b) schematic diagram of the zone-melting apparatus.

Aldrich) or Nichrome (diameter, about 0.3 mm), which generated a narrow molten zone in the organic film. The width of the molten zone was determined by the thickness of the substrate, the temperature, and the diameter of the heating wire and were in the range of 0.5–2.0 mm in our studies. The cell was then slowly moved at a fixed rate of 3, 6, 15, 30, 60, or 120 $\mu\text{m}/\text{min}$ with an inchworm motor (Burleigh) controlled by the same device that is used to move the electrode in a scanning electrochemical microscope. A monocular was used to observe the molten zone. In the operation, sometimes the heating wire needed to be tightened at high temperature to keep it straight and maintain a firm contact to the substrate. A slight bending of the heating wire would cause a deformation of the molten zone. All of the heating wires listed above worked well with the glass cells but not with the ITO ones, especially when the melting point of the compound studied was high and the ITO-coated glass was relatively thick (e.g., 0.9 mm) because the thinner wire was unable to raise the temperature high enough to melt the compound even after it was glowing red in the noncontact area. The temperature was raised slowly to avoid breaking the glass substrates. Pt wire was used instead of Nichrome only because it was more resistant to air oxidation and lasted longer.

The organic films were examined with an optical microscope (Olympus model BHTU) under ordinary or polarized light.

(5) Wright, J. D. *Molecular Crystals*, 2nd ed.; Cambridge University Press: Cambridge, 1995.

(6) Treggold, R. H. *Order in Thin Organic Films*; Cambridge University Press: Cambridge, 1994.

(7) Forrest, S. R. *Chem. Rev.* **1997**, *97*, 1793–1896.

(8) Liu, C.-Y.; Bard, A. J. *Acc. Chem. Res.* **1999**, *32*, 235–245.

(9) Gregg, B. A.; Fox, M. A.; Bard, A. J. *J. Phys. Chem.* **1990**, *94*, 1586.

(10) Liu, C.-Y.; Tang, H.; Bard, A. J. *J. Phys. Chem.* **1996**, *100*, 3587.

(11) Liu, C.-Y.; Lynch, V.; Bard, A. J. *Chem. Mater.* **1997**, *9*, 943.

(12) Fox, M. A.; Vincent, J. R.; Melamed, D.; Torimoto, T.; Liu, C.-Y.; Bard, A. J. *Chem. Mater.* **1998**, *10*, 1771–1776.

Photocurrent measurements were carried out in two different ways. First, a monochromator was placed in front of a halogen lamp (300 W) to generate a single wavelength light of 568 nm for porphyrin 1 and 586 nm for porphyrin 2. The two wavelengths correspond to the optical excitation of the ground state to the first singlet state for the two porphyrin molecules.¹² In another case, cells were fixed on the microscope stage and the light beam was focused to a desired size on a preselected domain of the film.^{1,10} The photocurrent was detected by a home-built high-sensitivity amplifier circuit or a CH Instruments (Austin, TX) model 660 electrochemical workstation. No external voltage bias was applied to the cells in any of the photocurrent measurements (i.e., they were short-circuit photocurrents).

Results and Discussion

1,4-Bis(butylamino)-9,10-anthraquinone. Differential scanning calorimetry of this material shows two peaks at 110.7 and 120.4 °C (melting point), indicating two phase transitions which could be seen as distinct colors with the naked eye. The capillary filling of SB35 from the molten state (~121 °C) into the cells of glass/SB35/glass produced thin, needle-shaped crystals that formed a fanlike structure shown in Figure 2a. Needles started from a center point and radiated in all directions; these were visible in ordinary light, polarized light, and with crossed polarizers. The deep color for one particular direction is the result of the irradiated light being polarized in that direction. The structure appeared similar to that seen with smectic liquid crystals.¹³ Note that when the cells were cooled quickly to room temperature after capillary filling, the fans became smaller but still had an identical overall structure. The smallest fan sizes observed with an optical microscope were of the order of tens of micrometers. The diameter of the individual needles was well below the resolution of an optical microscope and in the nanometer range. Films of different thickness, between 0.5 and 5 μm , showed the same appearance. By contrast, large area (approximately millimeter squared) single-crystal thin films were produced after the same films were recrystallized by the zone-melting technique through a single pass. The regrown films consisted of a number of single-crystal domains, each of which showed a single uniform color everywhere within the domain; the color changed systematically upon sample rotation with polarized light or between two crossed polarizers, as expected from a single crystal. A comparison of film structure before and after the zone-melting step is shown in Figure 2b. With this sample, the power to the heating wire was turned off when it was near the middle of the film. The regrown part of the film became a single crystal of uniform color while the quickly cooled recent molten zone and the rest of the crystal (area not melted) still showed fan structures. The grown single crystals were much larger and showed fewer structural defects compared to other organic films grown by an epitaxial technique.¹⁴ Note that if the whole cell with a single-crystal film was reheated to its molten state and slowly cooled, the film returned to the fan structure; this could be converted into a single-crystal thin film again after

another zone-melting process. Such a reversible evolution could be done a number of times without showing apparent changes in the film morphology.

The zone at the end of a zone-melting process showed smaller single crystals that were separated by some structures that appeared dark between two crossed polarizers (Figure 2c). These domains are either amorphous or consist of very small crystals in impurity-rich areas. In zone-melting, impurities, which are more soluble in the liquid than in the solid phase, are carried along the film in the direction of movement of the molten zone and are swept to the end of a sample.¹⁵ The impurity concentration in some areas could become sufficiently high to form impurity-rich domains that prevented single crystals from growing larger and could nucleate structural defects. Nevertheless, the near 90° corners and straight edges on the grown single crystals contrast remarkably with the fan-structure (Figure 2a). The growth rate had a strong effect on the crystal quality; in the 15–120 $\mu\text{m}/\text{min}$ range, a slower rate produced larger crystals with fewer defects. Since the interactions between the organic molecules are weak, a longer time may be required for molecules arriving at a growing crystal surface to attain their equilibrium positions and minimize the incorporation of impurity molecules and defects.

Single crystals should show better optical and optoelectronic properties (e.g., higher photoconductance, larger photocurrents, faster response) compared to amorphous and polycrystalline structures.^{8,10} We investigated this by examining the short circuit photocurrent, I_{sc} , with symmetrical sandwich cells containing organic molecular crystals, ITO/organic film/ITO, with irradiation.^{1,8–11,16–20} In this case, photogenerated electrons are preferentially injected into the irradiated ITO electrode from the excited molecules and holes move in the opposite direction to maintain a steady-state photocurrent across the whole film. Photoconductivity of the organic layer directly affects the charge carrier mobility and thus the photocurrent. In an amorphous or polycrystalline layer, charge trapping and detrapping at grain boundaries, structural defects, and impurity sites could slow the charge transport to a significant extent. This was indeed the case with the SB35 molecule, as shown in Figure 3. I_{sc} was over 1 order of magnitude larger from cells containing regrown single-crystal thin films than from those with needle-shaped crystals measured under identical conditions. In this experiment, ITO-coated glass replaced the glass coverslips as the substrate, but this did not affect the structure of the film. The cell was fixed on the stage of an optical microscope, and the light beam was focused on a spot of ~750 μm diameter in a specific single-crystal domain, as described earlier.¹ Essentially no variation was observed when the light beam was focused on different locations within the same domain or on similar domains within the polycrystalline films.

(15) Karl, N. *Mol. Cryst. Liq. Cryst.* **1989**, *171*, 157–177.

(16) Liu, C.-Y.; Pan, H.-L.; Fox, M. A.; Bard, A. J. *Science* **1993**, *261*, 897.

(17) Liu, C.-Y.; Pan, H.-L.; Fox, M. A.; Bard, A. J. *Chem. Mater.* **1997**, *9*, 1422.

(18) Liu, C.-Y.; Bard, A. J. *Chem. Mater.* **1998**, *10*, 840.

(19) Liu, C.-Y.; Pan, H.-L.; Tang, H.; Fox, M. A.; Bard, A. J. *J. Phys. Chem.* **1995**, *99*, 7632.

(20) Liu, C.-Y.; Bard, A. J. *J. Am. Chem. Soc.* **1998**, *120*, 5575.

(13) Gray, G. W.; Goodby, J. W. *Smectic Liquid Crystals*; Leonard Hill: Glasgow, 1984.

(14) Kobayashi, T. In *Crystals, Growth, Properties and Application 13, Organic Crystals I: Characterization*; Springer-Verlag: Berlin, 1991.



Figure 2. Micrographs of solvent blue 35 crystals between two pieces of glass (area of view, $0.28 \text{ mm} \times 0.49 \text{ mm}$). Top (a): Crystals grown by capillary filling irradiated with polarized light. Middle (b): Crystals first grown by capillary filling and then regrown with the zone-melting technique for upper-right portion (growth rate, $15 \mu\text{m}/\text{min}$) irradiated with polarized light. Bottom (c): Crystals regrown with the zone-melting technique (growth rate, $15 \mu\text{m}/\text{min}$) imaged between two crossed polarizers at a zone at the end of a pass.

Zinc(II) Meso-5,10,15,20-tetrakis-*n*-undecylporphyrin. *Film Growth.* As with SB35, porphyrin 1 also formed needle-shaped crystals arranged in a fanlike structure between two pieces of glass or ITO-coated glass upon capillary filling at its molten state ($131 \text{ }^\circ\text{C}$). The individual needles were too thin to be seen under ordinary light, but became visible between two crossed polarizers as shown in Figure 4a. This cell was placed on the heating wire and a molten zone was established. The well-ordered fanlike structure became highly irregular when the power to the heating wire was

suddenly turned off (Figure 4b), while the area that had not melted remained unchanged. Despite the differences in the initial morphology in different areas, the organic layer could be recrystallized into a single-crystal thin film after a single pass with the zone-melting technique at a scan rate of $15 \mu\text{m}/\text{min}$. A second pass at the same rate did not produce a significant difference in its appearance. However, a third pass at a lower rate of $6 \mu\text{m}/\text{min}$ caused the single-crystal domains to become larger with fewer apparent defects, as shown in Figure 4c. In this view, the white rectangular domains are

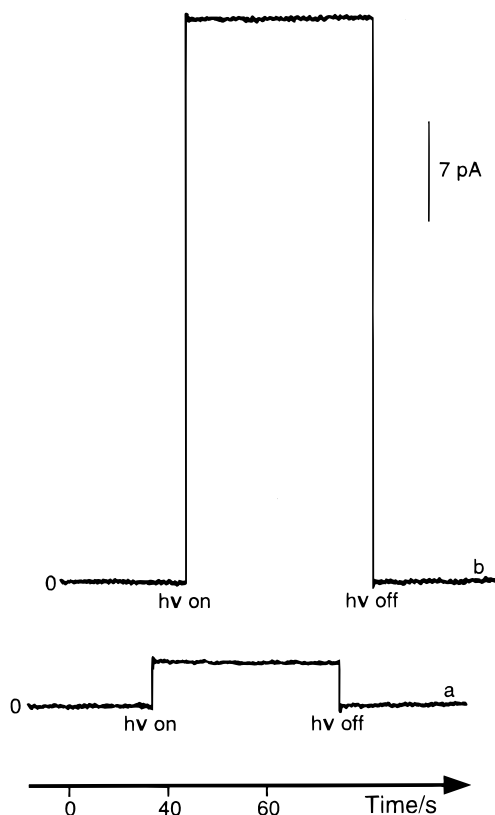


Figure 3. Short-circuit photocurrent as a function of time, generated with white light in (a) a needle-shaped polycrystalline film and (b) a regrown single-crystal domain under identical conditions. Irradiated spot, $750\ \mu\text{m}$ diameter. The zero current level is indicated in both curves (which are shifted for clarity).

actually air gaps formed during the film shrinkage as the temperature dropped from its molten state to room temperature. The dark straight horizontal lines were also air gaps that could be seen at higher magnification. This result again demonstrates the capability of the zone-melting technique to externally control the growth of organic single-crystal thin films. To the best of our knowledge, no other technique exists for growing a single-crystal film from an amorphous or microcrystalline film on a substrate such as glass or ITO. The simplicity of this zone-melting method contrasts to the technique of organic molecular beam epitaxy that is performed in an ultrahigh vacuum chamber on a single-crystal substrate.⁷ In the latter case, lattice matching is a prerequisite and an ordered structure can only be extended to a limited number of molecular layers (i.e., films of nanometer thickness).

Optoelectronic Properties. Photon-induced charge carriers traveling through an organic molecular crystal are frequently trapped and detrapped at defect sites including structure dislocations, grain boundaries, and impurities.^{16–18} It is therefore interesting to compare the charge transport properties in a thin film before and after the zone-melting treatment. Previous studies show that under certain conditions charge trapping and detrapping are reversible and can be externally controlled,^{16–18} and the same procedures could be used for studies of the porphyrin 1 molecule. For example, after the cell was charged under a bias voltage of $-0.2\ \text{V}$ (where the sign given always refers to the irradiated

ITO electrode) with irradiation at a wavelength of $568\ \text{nm}$ for $10\ \text{s}$ and kept in the dark under short-circuit conditions for $10\ \text{s}$, a discharge current, i.e., photocurrent spike, was observed when the charged cell was irradiated again with the same light without a bias voltage (short-circuit), as shown in Figure 5. In this case, parts a and b of Figure 5 were obtained from a cell showing either the fanlike structure (Figure 4a) or irregular morphology (Figure 4b), respectively. Thus, organic thin films with a polycrystalline structure have a high capability for charge trapping and detrapping. This conclusion is also true, as shown in Figure 6, when the same cell was charged under a positive bias of $+0.2\ \text{V}$, leading to a discharge current spike in a cathodic direction under short circuit. The responses in Figures 5a and 6a were obtained from the same spot on the sample, as were those in Figures 5b and 6b. However, after the same cell was subjected to a zone-melting treatment producing a single-crystal thin film, no discharge spike was seen after the sample was subjected to the same charging procedure under identical conditions (bias of $+0.2$ or $-0.2\ \text{V}$ with light at $568\ \text{nm}$). With these cells, the short-circuit photocurrent was essentially constant over time, implying that the charge trapping and detrapping, if any, must be too small to be seen in the single-crystal thin film of porphyrin 1. A comparison of steady-state I_{sc} obtained from cells showing different degrees of charge trapping and detrapping is shown in Figure 7. As expected, films that showed the highest extent of charge trapping and detrapping produced the lowest I_{sc} . Thus, a significant enhancement of the I_{sc} was achieved by the zone-melting process to produce improved quality and purity of the single-crystal thin film. The randomly distributed orientations of the tangled crystals were also perhaps shifted to a more favorable direction for the charge-carrier transport after the film was recrystallized into a single crystal.

Zinc(II) 2,3,7,8,12,13,17,18-Octa-*n*-decylporphyrin. Porphyrin 2 showed some complications in the zone-melting process. First it was difficult to see a molten zone in an ITO/porphyrin 2/ITO cell (while a clear color change was seen in the molten zone with porphyrin 1). Because porphyrin 2 has two phase transitions, at $117\ ^\circ\text{C}$ (from crystalline to mesophase) and $177\ ^\circ\text{C}$ (from mesophase to isotropic melt),¹² the change from a liquid crystal to an isotropic liquid is much less dramatic than that from a solid to liquid. To overcome this difficulty, the temperature inside the cells was calibrated by an Omegalable temperature monitor (Omega, Stamford, CT) sandwiched between the two ITO-coated glass slides and placed on the heating wire. The voltage to the wire was slowly increased until a temperature of $182\ ^\circ\text{C}$ was indicated and then the final voltage was applied for the zone-melting process. In this case, the width and uniformity of the molten zone were unknown, so a fine adjustment for the optimization of the molten zone could not be obtained. These films also often showed more than one structure at different locations before and after the zone-melting process. The domains with different morphology showed remarkably different optoelectronic properties. Therefore, a large number of cells were prepared for this study to obtain statistically significant results. This contrasts with cells of SB35 and porphyrin 1, where only one morphology dominated the

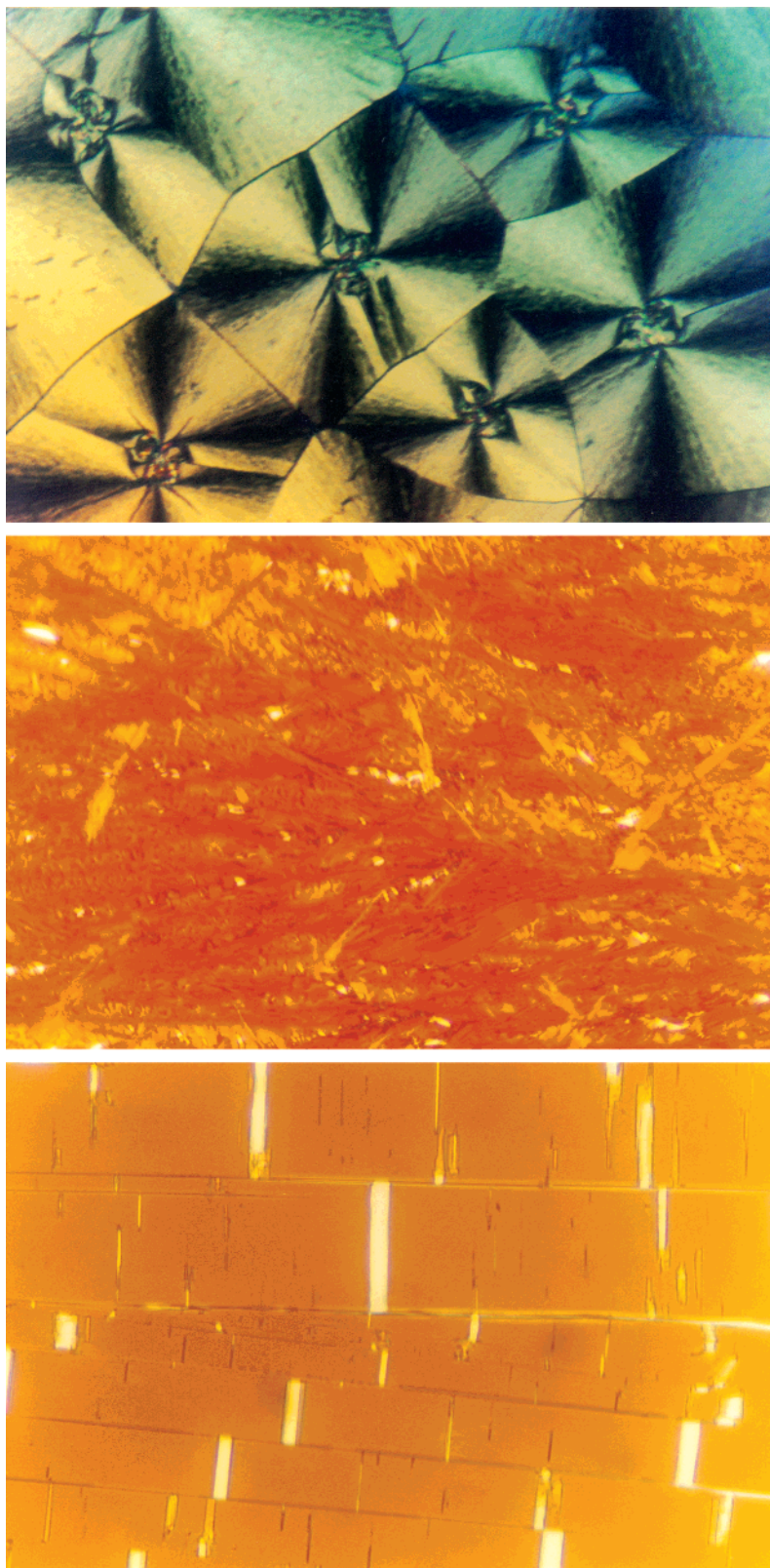


Figure 4. Micrographs of a porphyrin 1 thin film (area of view, $0.3 \text{ mm} \times 0.5 \text{ mm}$). Top (a): Crystals grown by capillary filling and imaged between two crossed polarizers. Middle (b): Crystals first grown by capillary filling and then remelted briefly with the heating wire and quickly cooled by turning the power off. Bottom (c): Crystals regrown by the zone-melting technique (growth rate, $6 \mu\text{m}/\text{min}$).

whole film (>90% area) before or after the zone-melting treatment, although somewhat different structures were also seen at few locations connected to the edge of the epoxy spacer. The varieties of morphology seen with the porphyrin 2 thin films may be related to the wide

temperature range of the liquid crystalline phase ($117\text{--}177 \text{ }^\circ\text{C}$) of this compound. Discotic liquid crystals are known to form at least six different structures.²¹ Because the molecules are still mobile at the liquid crystal phase, allowing self-organization, the rate of crystal

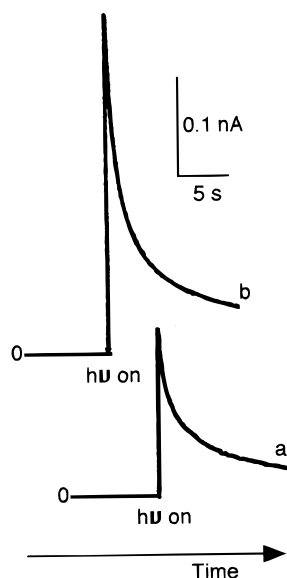


Figure 5. Short-circuit detrapping photocurrent of an ITO/porphyrin 1/ITO cell as a function of time by irradiation with 568-nm light. Charge was initially trapped under a bias of -0.2 V with a light at 568 nm for 10 s followed by a rest period of 10 s under short-circuit conditions in the dark; lines a and b were obtained from the areas shown in parts a and b of Figure 4, respectively.

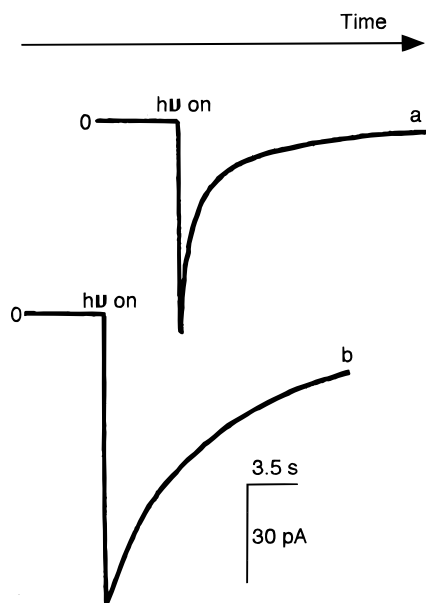


Figure 6. Short-circuit detrapping photocurrent of an ITO/porphyrin 1/ITO cell as a function of time, as in Figure 5 but under the initial bias of $+0.2$ V.

growth was probably lower than that of the other compounds, allowing formation of several different structures after the heating wire moved beyond the molten zone.

A few common morphologies of porphyrin 2 films are shown in Figure 8. The most striking feature is that many straight lines appeared in an organized pattern (Figure 8a). Such a structure could extend for several millimeters. Figure 9 shows the short-circuit photocurrent as a function of time generated from that area. In

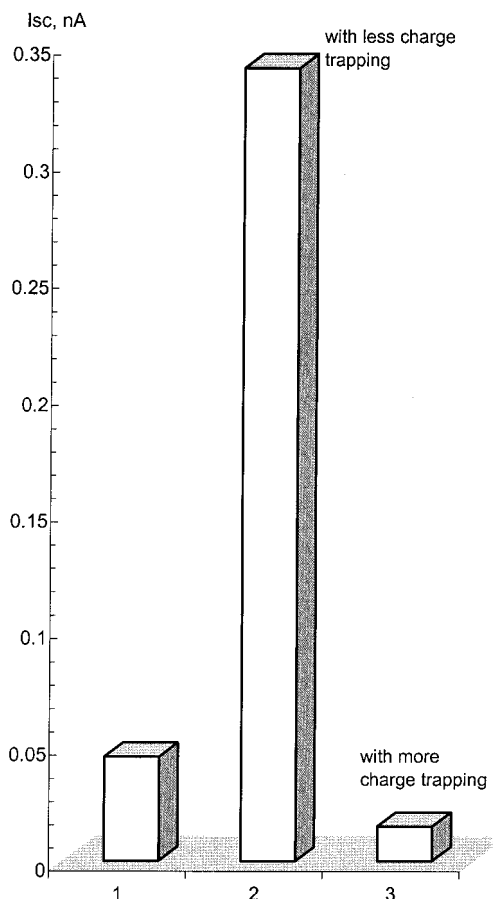


Figure 7. Steady-state short-circuit photocurrent of an ITO/porphyrin 1/ITO cell at three locations showing different levels of trapping capacity under identical experimental conditions. The highest photocurrent was obtained with the area processed by the zone-melting technique.

this case, light at a single wavelength of 586 nm irradiated the crystal through a hole (2.5 mm in diameter) on an Al plate attached firmly to both the surface of the sandwich cell and the exit of a monochromator. Anodic (or cathodic) I_{sc} spikes were produced when the light was chopped on (and off) and a steady-state I_{sc} was not seen. The organic thin film appeared to be insulating under irradiation, so the photogenerated charge carriers produced by exciton dissociation at the interface were unable to travel through the film, leading to a transient charge and discharge photocurrent. These straight lines in Figure 8a appeared black between two crossed polarizers as examined under an optical microscope, indicating an amorphous structure that does not show good charge carrier transport properties.

Figure 8b shows two neighboring domains in which the right portion is similar to that in Figure 8a; the straight lines were slightly thinner but were clearly seen at high magnification. The left portion was a crystalline structure which sharply contrasts to the domain on the right when examined between two crossed polarizers (Figure 8c). Although the crystal appeared to be of poor quality, the left domain generated a steady-state I_{sc} that was essentially constant over time for 30 min and no photocurrent spikes were observed when the light was chopped on and off. In the dark domain at right, however, I_{sc} vs t was similar to that shown in Figure 9,

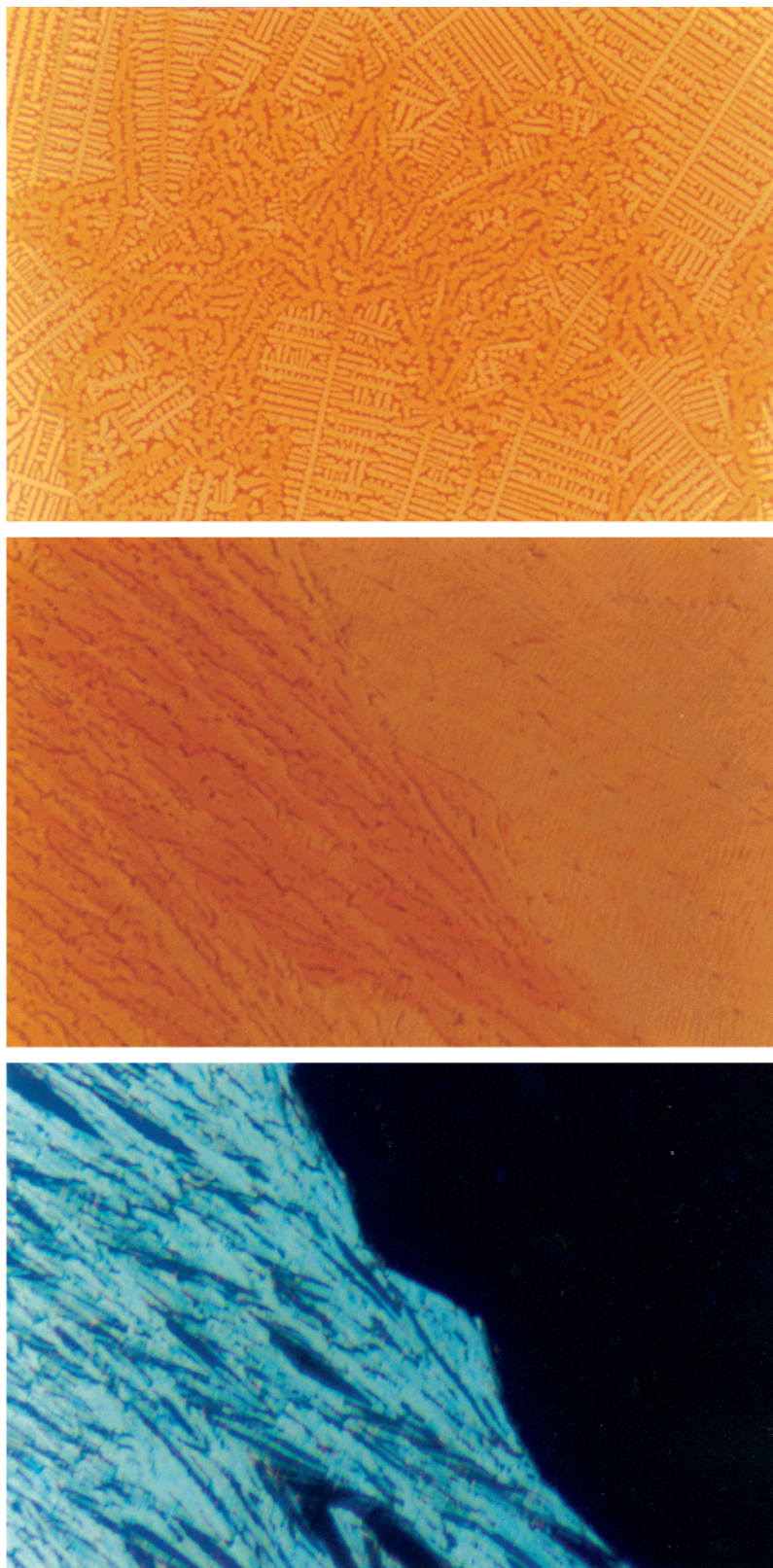


Figure 8. Micrographs of a porphyrin 2 thin film grown by capillary filling (area of view, $0.3 \text{ mm} \times 0.5 \text{ mm}$). Top (a) and middle (b): Imaged without polarizer at two different locations. Bottom (c): Imaged between two crossed polarizers at the same location as in b.

except that the charge and discharge photocurrent decayed more slowly. Previously, we have studied the effect of structure order on charge-carrier transport through thin-layer cells of ITO/ZnODEP/ITO¹⁹ by monitoring the current flow as a function of temperature. The current dropped sharply at the melting point when

the crystal structure changed into a disordered isotropic liquid, while the current increased suddenly during cooling when the randomly oriented ZnODEP molecules in the liquid state reordered into a regular molecular crystal at the transition to mesophase. The electrically conducting molecular stacks between the two electrodes

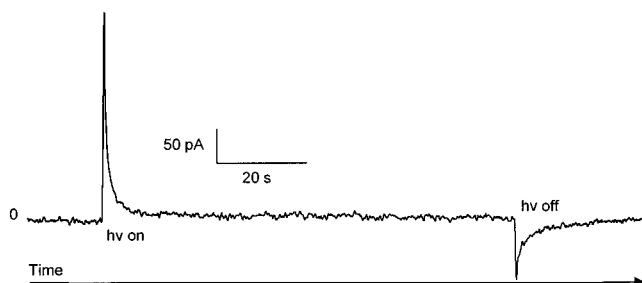


Figure 9. Short-circuit photocurrent as a function of time for a porphyrin 2 cell with irradiation at 568 nm at the area shown in Figure 8a. Irradiated spot is 2.5 mm in diameter.

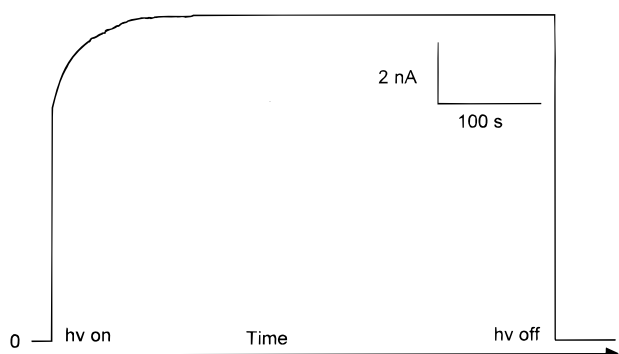


Figure 10. Short-circuit photocurrent as a function of time for a porphyrin 2 cell with irradiation at 568 nm from a regrown crystal domain. Irradiated spot is 2.5 mm in diameter.

switched on and off when the molecules were reversibly changed between ordered and disordered structures at the melting point. Such an effect was even more clearly seen in the present study where the disordered (amorphous) and the ordered structures were all in the same solid state.

After recrystallization by the zone-melting process, the single-crystal thin films produced were similar to those in Figure 4c. In these, the steady-state I_{sc} increased significantly, as shown in Figure 10, compared to those produced under identical experimental conditions (shown in Figure 9). Such a dramatic improvement in the I_{sc} generation demonstrates again the value of the zone-melting technique. Figure 11 shows the steady-state I_{sc} obtained from different domains in the same or different cells. In these measurements, cells were fixed on the stage of the optical microscope whose light source was used for irradiation through the objective. Each domain was first examined with polarized light, but the photocurrent measurement was obtained without a polarizer.^{1,10} The amorphous domains produced a near-zero photocurrent, while the single-crystal domains generated the largest I_{sc} . Between these two extremes, intermediate I_{sc} values were obtained from polycrystalline domains, in which the crystal orientation may play an important role,^{1,10} in addition to the grain boundary effect in slowing down the charge carrier transport. As in the case of porphyrin 1 shown above, more charge trapping occurred with the polycrystalline domains than with the single-crystal ones.

Because the zone-melting technique can also purify the materials during the crystallization, the large area single-crystal thin films should be purer than the original films. This higher purity may be a factor in the

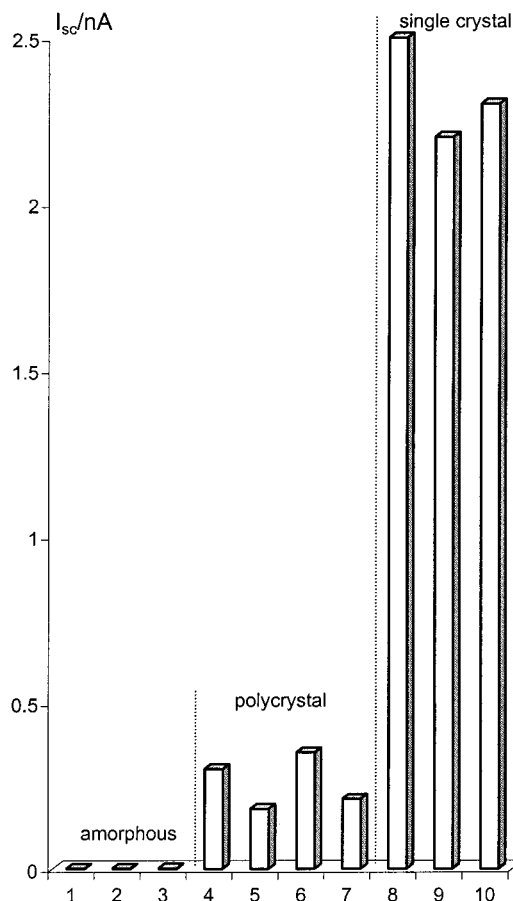


Figure 11. Steady-state short-circuit photocurrent of a porphyrin 2 cell at different locations showing different levels of crystallinity under identical experimental conditions. Irradiated spot is 300 μm in diameter.

formation of the large single-crystal thin films. To test this assumption, a number of cells were processed with several passes of zone melting, the hypothesis being that as the film was made purer after consecutive passes, the crystal domain should become larger. Such a relationship, however, was not observed. Moreover, the photocurrent response did not generally improve with the total number of passes.

On the other hand, the film morphology at some locations in contact with the epoxy cement used as a spacer was somewhat different from that in other areas, and the structure of the recrystallized films depended on whether the epoxy spacer in a cell was initially aligned parallel or perpendicular to the heating wire for porphyrin 2. In the parallel case, the epoxy would influence the initial crystallization in the first molten zone, while in the perpendicular orientation, the epoxy existed only at the two ends (Figure 1b), indicating that the first crystal structure (the seed crystal) was important. Thus, the zone-melting technique is probably a primarily single-crystal growth method resembling the traditional pulled crystal growth technique, during which the impurities are rejected by the growing solid and accumulate in the liquid moving slowly toward the other end. This conclusion is supported by the fact that the fanlike structure (SB35) reappeared after films formed by the zone-melting process, which produced single-crystal thin films, were uniformly heated again

to the melting point briefly and then cooled to room temperature. In this case it was unlikely that the impurities accumulated at the end would spread fast enough to affect the whole film.

Conclusion

The simultaneous growth and purification of organic single-crystal thin films led to a large improvement of the optoelectronic properties. This simple zone-melting technique offers a convenient way to prepare films of molecular materials for possible applications in optics and electronics.²²⁻²⁴

Acknowledgment. We thank Dr. Dan Melamed for his syntheses of the two porphyrins. The support of this work by the National Science Foundation (CHE9876855) and the Robert A. Welch Foundation is gratefully acknowledged.

CM000353X

(22) Sheats, J. R.; Antoniadis, H.; Hueschen, M.; Leonard, W.; Miller, J.; Moon, R.; Roitman, D.; Stocking, A. *Science* **1996**, *273*, 884-888 and references therein.

(23) Liu, C.-Y.; Pan, H.-L.; Bard, A. J.; Fox, M. A. U.S. Patent 5327373.

(24) Liu, C.-Y.; Hasty, T.; Bard, A. J. *J. Electrochem. Soc.* **1996**, *143*, 1916.